

ORIGINAL ARTICLE

miR-200a regulates Rheb-mediated amelioration of insulin resistance after duodenal–jejunal bypass

W Guo, H Han, Y Wang, X Zhang, S Liu, G Zhang and S Hu

OBJECTIVES: Duodenal–jejunal bypass (DJB) surgery can induce the rapid and durable remission of diabetes. Recent studies indicate that ameliorated hepatic insulin resistance and improved insulin signaling might contribute to the diabetic control observed after DJB. Ras homolog enriched in brain (Rheb) is reported to have an important role in insulin pathway, and some microRNAs (miRNAs) have been found to regulate Rheb. This study was conducted to investigate the effects of DJB on hepatic insulin resistance and the effects of miRNA-200a, a Rheb-targeting miRNA, on the development of DJB-induced amelioration in hepatic insulin resistance.

SUBJECTS: We investigated hepatic insulin signaling change and mapped the hepatic miRNAome involved in a rat model of DJB. We studied the effects of miR-200a on Rheb signaling pathway in buffalo rat liver cell lines. Liver tissues were studied and glucose tolerance tests were conducted in DJB rats injected with lentivirus encoding miR-200a inhibitor and diabetic rats injected with miR-200a mimic.

RESULTS: Rheb is a potential target of miR-200a. Transfection with an miR-200a inhibitor increased Rheb protein levels and enhanced the feedback action on insulin receptor substrate-dependent insulin signaling, whereas transfection with an miR-200a mimic produced the opposite effects. A luciferase assay confirmed that miR-200a bind to the 3'UTR (untranslated regions) of Rheb. Global downregulation of miR-200a in DJB rats showed impaired insulin sensitivity whereas upregulation of miR-200a in diabetic rats showed amelioration of diabetes.

CONCLUSIONS: A novel mechanism was identified, in which miR-200a regulates the Rheb-mediated amelioration of insulin resistance in DJB. The findings suggest miR-200a should be further explored as a potential target for the treatment of diabetes.

International Journal of Obesity (2016) 40, 1222–1232; doi:10.1038/ijo.2016.60

INTRODUCTION

Diabetes and its co-morbidities have reached epidemic proportions across the developed and developing world, imposing an unsustainable socioeconomic burden on many societies.¹ Bariatric surgery induces a profound and durable amelioration of diabetes mellitus (DM) and has undergone steady growth worldwide. Duodenal–jejunal bypass (DJB) bypasses the proximal segments of the small bowel (duodenum and jejunum) and expedites delivery of nutrients to ileum. Experimental evidence from animals suggest that the improvement of diabetes after DJB is independent of weight loss. Possible weight-independent mechanisms include changes in gut hormones, bile acid metabolism, nutrient sensing,² microbiota^{3,4} and insulin sensitivity.

Liver, the main glucose-utilizing organ, has a large role in systemic glucose homeostasis. Accumulating evidences implicate that restored hepatic insulin signal transduction might contribute to insulin resistance amelioration as well as DM remission after DJB.^{5,6} Ras homolog enriched in brain (Rheb), a member of the Ras-like family of GTPases, is an essential component of the insulin signaling pathway. The Rheb/mTOR cassette is usually augmented in insulin hypersufficiency and a low sensitivity of glucose-utilizing organs to insulin.^{7,8} Rheb/mTOR signaling constitutively engages a negative feedback mechanism that regulates insulin receptor substrate (IRS) phosphorylation, and leads to the downregulation of downstream mediators of the insulin pathway, which is termed insulin resistance *in vivo*.

With the discovery of microRNAs (miRNAs), research on Rheb regulation has progressed and several miRNAs have been found to regulate Rheb in various tissues and disease conditions. miRNAs are endogenous, small non-coding RNAs of approximately 19–22 nucleotides in length, which anneals inexactly to complementary sequences in the 3'-untranslated regions (3'UTRs) of target mRNAs to either facilitate their degradation or repress the translation process.⁹ miRNAs regulate thousands of genes at the post-transcriptional level and each miRNA can potentially target several mRNAs.¹⁰ miRNAs may play a role in many biological processes including the development of metabolic diseases such as diabetes.^{11–19}

It is reported that some miRNA could elicit different biological effects by targeting Rheb. miR-155 could suppress the macrophage-mediated bacterial phagocytosis in bacterial keratitis²⁰ and regulate autophagy-mediated mycobacterial elimination by targeting Rheb.²¹ Although some research has been conducted on miRNA-mediated regulation of Rheb in various physiological and pathological conditions, no studies have been conducted on such regulation in DM and DJB. In this study we investigated the role of a specific miRNA, miR-200a, in regulating Rheb after DJB. As Rheb is a possible target of miR-200a (www.mirdb.org), we explored this relationship further in DM and DJB. We hypothesized that following DJB, the individual establishes a new metabolic balance via the manipulation of miR-200a. We investigated whether miR-200a alteration occurs in DJB, and

whether such alterations cause insulin resistance amelioration as well as DM remission after DJB.

MATERIALS AND METHODS

Animals

Eight-week-old male Wistar rats (180–200 g) were purchased from the Laboratory Animal Center of Shandong University (Jinan, China). The rats were housed in individual cages under controlled temperature ($24 \pm 2^\circ\text{C}$), humidity and lighting (12-h light/dark cycle with light at 0700 hours). Thirty rats had free access to a high-fat diet (40% of the calories as fat, Huabukang Biotech Company, Beijing, China) and tap water for 4 weeks to induce insulin resistance, followed by intraperitoneal injection of Streptozotocin (STZ; 35 mg kg^{-1}) to induce hyperglycemia. Three days later, random blood glucose was measured in duplicate from tail vein blood using a glucometer (Roche One Touch Ultra, Lifescan, Johnson & Johnson, Milpitas, CA, USA). Rats with random blood glucose $\geq 11.1 \text{ mmol l}^{-1}$ and random serum insulin level are within $0.5\text{--}1.5 \text{ ng ml}^{-1}$ were considered diabetic and selected for further studies ($n = 35$), and the rats with random blood glucose $\geq 11.1 \text{ mmol l}^{-1}$ and random serum insulin level are lower than 0.5 ng ml^{-1} were excluded. The rats are randomly allocated to different groups and investigators are totally blinded to the allocation. The study was approved by the Animal Care and Utilization Committee of Shandong University and informed consent was obtained.

Surgical techniques

All rats were fed a non-residue diet for 2 days and were fasted overnight pre-operatively. During surgery, the rats were anesthetized with 10% chloral hydrate solution. DJB ($n = 15$) involved (1) a 4-cm midline epigastric incision, (2) transection of the duodenum distal to the pylorus and suture of its proximal end using 7-0 silk suture (Ningbo Medical Needle, Ningbo, China), (3) transection at the plane of the distal jejunum (10 cm from the ligament of Treitz), (4) connecting the distal limb to the pylorus and (5) a jejunojejunal anastomosis (connecting the proximal limb with the jejunum at 10 cm distally). Sham surgeries involved the same abdominal incisions and gastrointestinal transections. However, no removal was made, and all reanastomosis was performed at the same sites as in the DJB procedures. In addition, the operation time of the rats in the sham group was prolonged to obtain similar operative stress to that of the rats in the DJB group. All animal experimental protocols were in accordance with the National Institute of Health standards and were approved by the Animal Care and Utilization Committee of Shandong University.

Sleeve gastrectomy (SG; $n = 5$) surgery involved (1) a 4-cm midline epigastric incision, (2) dissecting the gastric omentum and disclosing the gastric cardium, (3) ligating and transecting short gastric vessels, related gastroepiploic vessels and the branches of left gastric vessels in the greater curvature using 7-0 silk suture (Ningbo Medical Needle), (4) removing the gastric fundus and a large portion of the gastric body and (5) closing the residual stomach using 7-0 silk suture (Ningbo Medical Needle).

Hormones

At 8 weeks post operation, blood samples were collected from the angular vein of anesthetized rats at 30, 60 and 120 min after 1 g kg^{-1} glucose gavage. After centrifuging (1000 *g*) the blood at 4°C for 15 min, the serum was immediately extracted and stored at -80°C . Insulin secretion was measured using enzyme-linked immunosorbent assay (ELISA) kits (Millipore, MA, USA). Glucagon-like peptide 1 (GLP-1) was measured using ELISA kits (Uscn Life Science, Wuhan, China).

Oral glucose tolerance test

An oral glucose tolerance test (OGTT) was performed at 8 weeks after surgery and 2 weeks after transfection. Blood glucose was measured using a glucometer (Roche One Touch Ultra, Lifescan, Johnson & Johnson, Milpitas, CA, USA) in conscious rats at baseline and at 30, 60 and 120 min after the administration of 1 g kg^{-1} glucose by oral gavage using.

Insulin tolerance test

An insulin tolerance test (ITT) was performed at 8 weeks post operation and 2 weeks post transfection by measuring glucose levels at baseline and

at 30, 60 and 120 min after the injection of 0.5 IU kg^{-1} human insulin intraperitoneally in conscious and fasted rats.

Western blotting

All rats were sacrificed at 9 weeks after operation. The liver was rapidly removed, immediately frozen in liquid nitrogen and stored at -80°C until analysis. Proteins were detected using the following antibodies: anti-RHEB, anti-mTOR, anti-mTOR (phospho S2448), anti-IRS1, anti-IRS1 (phospho Y896), anti-IRS2, anti-IRS2 (phospho Y911 and S303) anti-AKT, anti-AKT (phospho S473; Abcam, MA, USA) and anti-GAPDH (Santa Cruz, CA, USA).

Immunohistochemistry

Tissue samples were cut from the liver and fixed in 4% formaldehyde. Tissue samples were embedded in paraffin and were reacted with rabbit anti-rat Rheb polyclonal antibody (Abcam). The sections were incubated with a goat anti-rabbit peroxidase-labeled secondary antibody (ZSGB-BIO) for 15 min. A computer-assisted morphometric analysis system (Image-Proq1 Plus 5.0, Media Cybernetics, Rockville, MD, USA) was used for histopathological analysis of the slides. The mean integrated optical density value of positive staining of Rheb in the liver was analyzed using Image-Pro Plus.

MicroRNA qPCR array

The miProfile Customized Rat qPCR Arrays (GeneCopoeia, Rockville, MD, USA) 96-well-qPCR plate was used for this study. Each array is a panel of validated, optimized qPCR primers for 84 miRNAs closely associated with diabetes, and the housekeeping genes 5S rRNA and RsnRNA U6, which are used as reference factors to normalize the expression results. Each well contains a forward primer for the mature miRNA sequence and a universal adaptor reverse primer cross-linked to the 96-well plate. The qPCR Primer Array was performed in 20 μl reaction volumes containing 1 μl reverse transcription product, according to the manufacturer's instructions using SYBR Green detection on the ABI 7900HT instrument (Applied Biosystems, Carlsbad, CA, USA). The 84 diabetes-related microRNA are confirmed according to 11 diabetes-oriented experimental papers.^{22–32}

mRNA extraction and quantitative analysis

RNA was isolated using TRIZOL (Invitrogen, Burlington, ON, Canada). Real-time RT-PCR was performed using a ReverTra Ace qPCR RT Kit (TOYOBO, Shanghai, China) and a Qiagen One Step RT-PCR kit with a custom-made Rheb primer and a LightCycler (Roche Diagnostics, Laval, QC, Canada) instrument. The data were normalized to GAPDH mRNA. RT-PCR was conducted in a reaction volume of 20 μl .

Transfection with miRNA mimic or inhibitor

Buffalo rat liver (BRL) cells were ordered from ATCC (product no. CRL-1442) and it was authenticated and tested for mycoplasma contamination. BRL cells were transfected with an miR-200a mimic or an miR-200a inhibitor (60 nmol l^{-1} ; Biosune, Shanghai, China) using Lipofectamine 2000 (Invitrogen). Scrambled controls were used in parallel. To construct insulin-resistant BRL cell model, Cells were cultured in the presence of a high concentration of insulin (1000 nM) for 24 h with complete medium, followed by 30 min without insulin as well as fetal bovine serum in the medium. Then cells were cultured in 1000 nM insulin for 5 min with complete medium and the insulin-resistant BRL cell line is established. BRL cells were transfected with an miR-200a mimic and inhibitor or its corresponding negative control. Forty-eight hours later, the cells were starved in Krebs-Ringer bicarbonate HEPES medium for 2 h and either were or were not stimulated with 100 nmol l^{-1} insulin for 10 min.

Luciferase reporter assay targeting Rheb-3'UTR

Rheb cells were co-transfected with one of the following reporter luciferase vectors (Genechem, Shanghai, China): a vector containing the 3'UTR Rheb oligonucleotides that are predicted to interact with miR-200a or vector containing a mutated sequence. The cells were also transfected with either a negative control mimic or an miR-200a mimic using of Lipofectamine 2000 (Invitrogen). Forty-eight hours after transfection, the cells were assayed for firefly luciferase and Renilla luciferase activity using a Dual-Luciferase Reporter Assay System (Promega, Madison, WI, USA) and renilla luciferase activity was used as an internal control.

Transgenic rat model construction after DJB

Rats were randomly divided into two groups for lentivirus treatment ($n=5$ each): (1) DJB+green fluorescent protein: injection of a lentivirus vector encoding a green fluorescent protein reporter via the rat tail vein²⁸ as a negative control for 7 days; (2) DJB+miR-200a inhibitor: Injection of lentivirus vector encoding miR-200a inhibitor via the tail vein for 7 days. Liver tissues were collected, snap frozen and stored at -80°C until further analysis.

Statistical analysis

Values are expressed as the means \pm s.d. for each condition and were analyzed using SPSS software 17.0 (Chicago, IL, USA). Continuous variables were compared among multiple groups using one-way ANOVA (analysis of variance), and *post hoc* comparisons were made using limited slip differential at homogeneity of variance or Dunnett's T3 at heterogeneity of variance. Two-tailed $P < 0.05$ was considered to represent statistical significance.

RESULTS

Body weight, calorie intake, glucose metabolism and serum hormones parameters study

Following DJB on diabetic rats induced by high-fat diet (HFD) and STZ, we did not find any difference in *ad libitum* blood glucose levels between DJB ($n=5$) and sham($n=5$) until 4 weeks after DJB. Thereafter, the DJB group showed lower *ad libitum* blood glucose levels than the sham group, and this difference became more evident from 4 weeks after surgery and persisted until 8 weeks after surgery (Figures 1a and b). Body weight gain was slightly attenuated only during the early postoperative period in the DJB group compared with the sham group (Figure 1c). Calorie intake was comparable between sham and DJB groups at all measuring time points (Figure 1d). OGTTs and ITTs were performed at weeks

2 and 4 after surgery. There is no significant alteration of OGTT, ITT, and serum insulin and GLP-1 level during OGTT 2 weeks after DJB (Figure 1e). However at week 4 after DJB, the post-prandial blood glucose level at all measuring time points after glucose challenge was significantly lower in the DJB group than in the sham group (Figure 1f). Insulin sensitivity (assessed using an ITT) indicated an improvement in systemic insulin sensitivity in the DJB groups at week 4 (Figure 1f). During the OGTT, no alteration of plasma insulin levels was observed in the DJB group at week 4; in contrast, plasma GLP-1 levels were mildly elevated in the DJB group (Figure 1f).

Differentially expressed miRNAs in the liver of control, DM and post-DJB Wistar rats

To identify whether miRNAs are differentially expressed in the liver with DJB ($n=4$) and Sham ($n=4$) operation in diabetic Wistar rats induced by HFD and STZ, we conducted an initial screening of diabetes-related miRNAs (Figure 2a). We collect the liver tissue at fed state 8 weeks after DJB or Sham operation. In DM, 84 miRNAs have been found to be differentially expressed during insulin resistance and diabetes progression according to a series of experimental study conducted on microRNAs change.²²⁻³² We found 12 miRNAs that were highly significantly dysregulated (based on a two-tailed Student *t*-test $P < 0.01$) in post-DJB diabetic rats compared with sham-operated rats; all 12 miRNAs were upregulated (miR-29a-3p, miR-194-5p, miR-30c-5p, miR-27a-3p, miR-23b-3p, miR-365-3p, miR-200a-3p, miR-26b-5p, miR-29c-3p, miR-24-3p, miR-130-3p and miR-let-7i-5p). The clustered miRNA profiles show a relatively clear differentiation between the DJB and SHAM groups: the DJB-altered microRNAs typically exhibited a 1.9- to 4.6-fold change compared with sham-operated rats (Figure 2b).

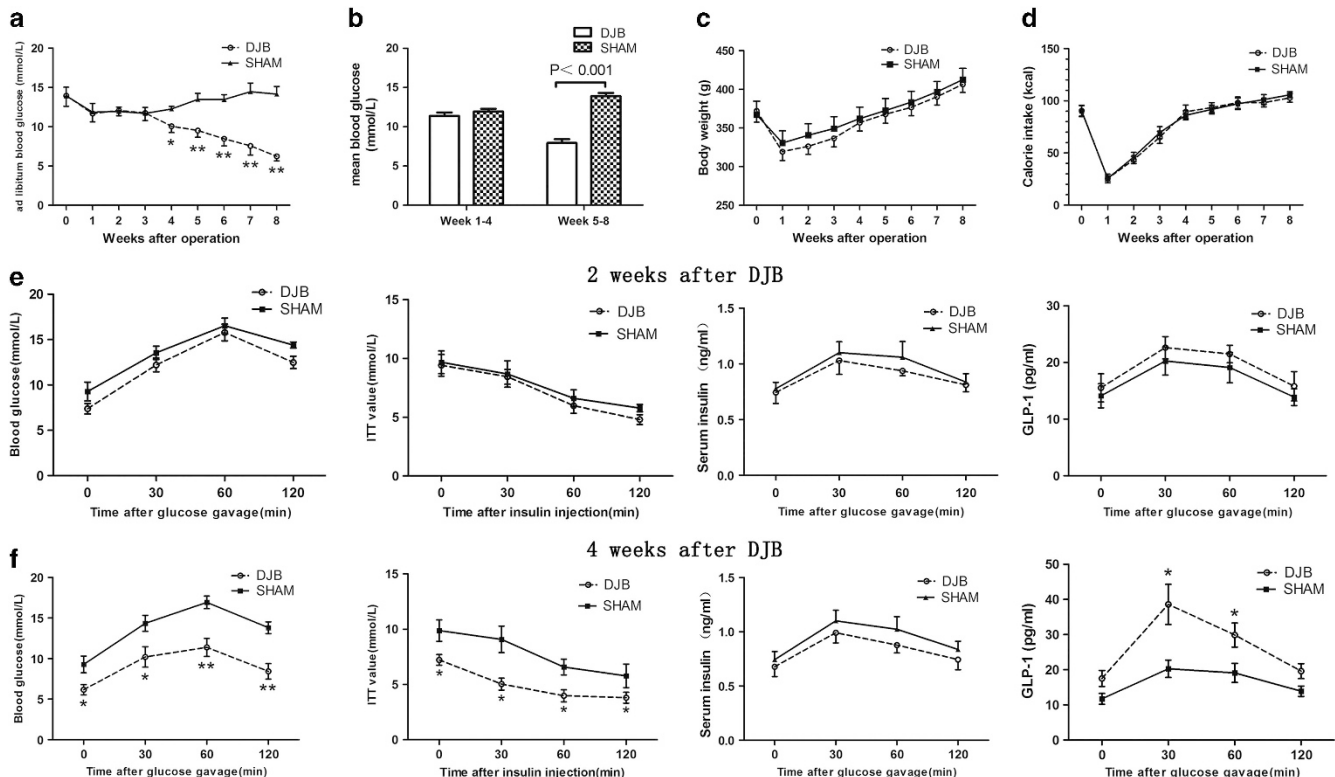


Figure 1. (a) Blood glucose levels in diabetic Wistar rats after surgery. Blood glucose levels were measured under fed conditions at 0900 hours. (b) Mean blood glucose levels during the early (1–4 weeks) and late (5–8 weeks) postoperative periods. (c, d) Body weight and calorie intake were measured each week for 8 weeks postoperatively. (e, f) Blood glucose, plasma insulin and GLP-1 levels during OGTT and ITT at 2 and 4 weeks after surgery. Data are presented as the means \pm s.e. ($n=5$ for each group). * $p < 0.05$, ** $p < 0.01$ according to the *t*-test, and variance between each group is similar.

Among the 12 miRNAs that are expressed at highly significantly changed levels, miR-200a is the one that has been predicted to target Rheb. Three softwares have been used for the

prediction (<http://www.targetscan.org>, <http://www.microrna.org> and <http://mirdb.org>). The predicted miR-200a binding site in the 3'UTR of Rheb mRNA is phylogenetically maintained, suggesting

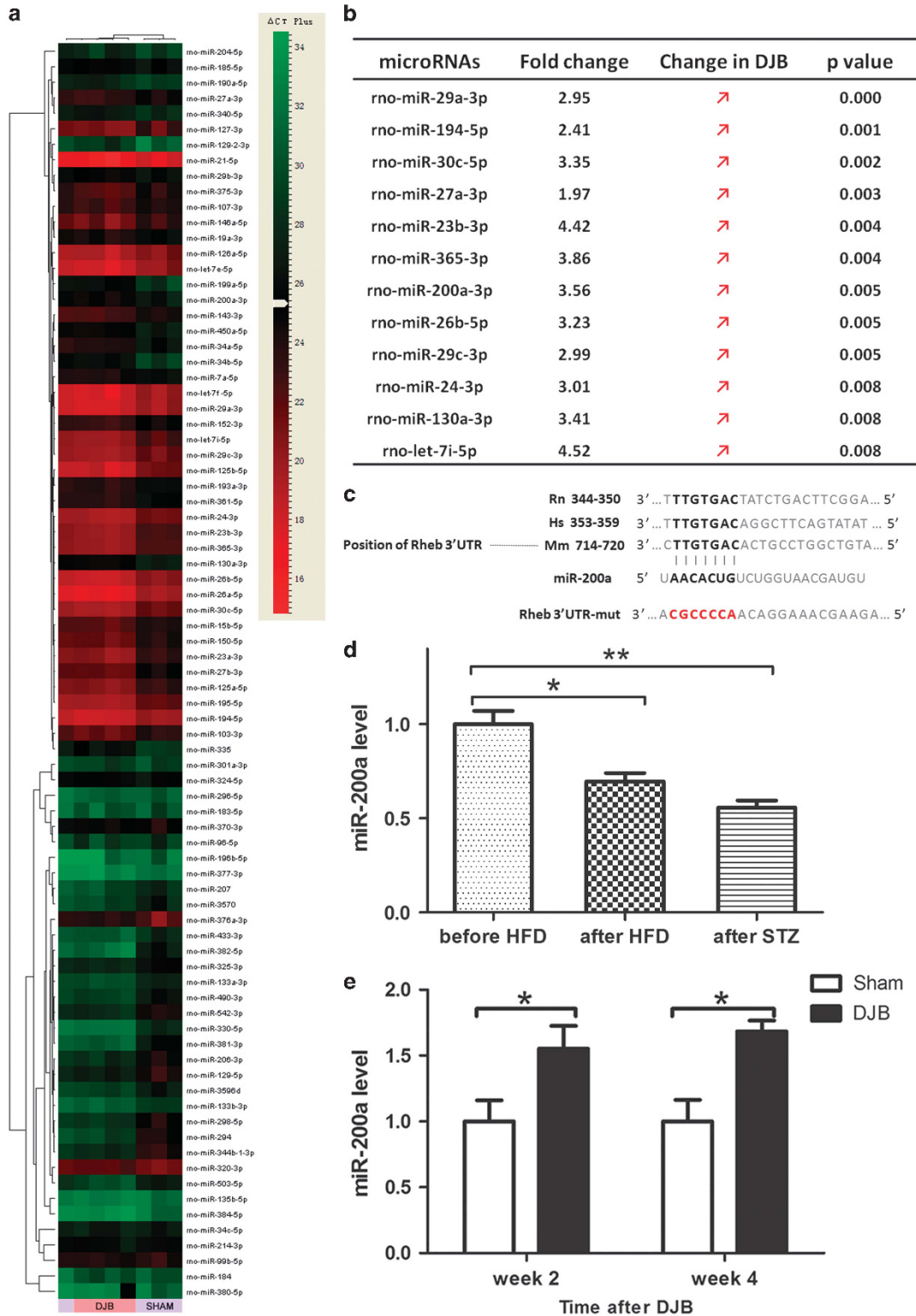


Figure 2. (a) A heat map of hepatic microRNA with two-way clustering showing a relatively clear grouping of DJB and SHAM animals based on 84 diabetes-related microRNAs. (b) DJB altered the hepatic expression of 12 miRNAs ($P < 0.01$), all of which were upregulated in the DJB-operated animals ($n = 4$) compared with the sham controls ($n = 4$). P -values using a two-tailed t -test. (c) Scheme of the interaction between miR-200a and the 3'UTR of rat, human and mouse Rheb. (d) The expression of miR-200a during the induction of DM. (e) Differential expression of miR-200a in liver 2 weeks and 4 weeks after DJB. Error bars represent the experimental s.d. and variance between each group is similar. $*P < 0.05$, $**P < 0.01$ according to the t -test.

that the function of miR-200a as a potential regulator of Rheb has been conserved in mice, rats and humans (Figure 2c). Then expression of miR-200a during diabetes induction is studied (Figure 2d). MiR-200a was decreased by 30% in the liver of after-HFD rats (at the end of 4-week induction with HFD, $n=5$) compared with before-HFD rats ($n=5$) at fed state. Three days after STZ injection, hepatic miR-200a expression ($n=5$) reduced 45% compared with before-HFD rats at fed state. MiR-200a in the liver of diabetic rats induced by HFD and STZ is much less abundant than non-diabetic normal control animals. To elucidate the significance of miR-200a, we measured the hepatic miR-200a level at week 2 ($n=5$) and week 4 ($n=5$), showing that both were significantly elevated compared with sham group (Figure 2e). This indicated that alteration of miR-200a level was previous to alteration of glucose metabolism.

DJB causes the Rheb-mediated amelioration of insulin resistance
We detected both the phosphorylated and total protein levels of the key mediators of this pathway in diabetic rats after DJB and sham. At 8 weeks postoperatively, western blot shows that hepatic Rheb/mTOR cassette was significantly downregulated in the DJB group compared with the sham group; the tyrosine phosphorylation levels of IRS1/2 and serine phosphorylation of AKT were higher in the DJB group (Figure 3a). Serine phosphorylation of IRS2, which is believed to regulate hepatic insulin sensitivity, seems unchanged according to the western blot. Immunohistochemistry (IHC) confirmed an obvious decrease of Rheb in the liver of DJB group 8 weeks after surgery (Figures 3b and c). Phosphoenolpyruvate carboxykinase (PEPCK) and G6Pase, which regulate the hepatic gluconeogenesis, are downregulated in liver of DJB group using qPCR (Figure 3d).

miR-200a regulates Rheb protein levels

Rheb is one of the predicted targets of miR-200a. The mimic increased miR-200a levels by 300 fold (Figure 4a), and the inhibitor reduced miR-200a levels by 60% (Figure 4b). MiR-200a over-expression in BRL cells resulted in a 65% reduction of Rheb mRNA and 33% reduction in Rheb protein levels; in contrast, decreased levels of miR-200a increased the levels of Rheb mRNA and protein by 50% and 33%, respectively (Figures 4c–e). To evaluate whether the predicted miR-200a target site in the 3'UTR of Rheb mRNA was directly involved in the miR-200a-induced change in Rheb protein levels, we cloned the putative 3'UTR target site downstream of a luciferase reporter gene and co-transfected the p-Luc-3'UTR Rheb construct into BRL cells together with either miR-200a mimic and negative control mimic. The luciferase activity of cells that had been transfected with miR-200a and p-Luc-3'UTR Rheb was decreased by 60% compared with cells that had been co-transfected with control and p-Luc-3'UTR Rheb (Figure 4f). Taken together, our data argue that miR-200a and Rheb mRNA interact directly.

miR-200a decreases downstream of Rheb and upregulates the IRS1-dependent insulin signaling

We first established an *in vitro* model of insulin resistance. To study the effect of miR-200a on insulin signaling in an insulin-resistant BRL cell line, we examined the phosphorylation state of molecules functioning downstream of Rheb using transfection of miR-200a mimic, inhibitor, negative control mimic and negative control inhibitor. Western blotting analysis showed that mTOR phosphorylation were less abundant in cells overexpressing miR-200a than in controls, thus causing high tyrosine phosphorylation of IRS1/2 and serine phosphorylation of AKT (Figure 5a). In contrast, miR-200a inhibitor transfection caused high mTOR phosphorylation and restrained the tyrosine phosphorylation of IRS1/2 and serine phosphorylation of AKT. The serine phosphorylation of IRS2 remain unchanged when subjected to miR-200a mimic and inhibitor compared with each negative control (Figure 5a). We also found

that the high expression of miR-200a resulted in more potent enhancement of the AKT phosphorylation level in response to insulin stimulation, whereas transfection with a miR-200a inhibitor did not significantly change the phosphorylation level of AKT (a crucial mediator of insulin functioning) (Figure 5b). Also we conducted the same insulin stimulation on normal BRL cell line after transfection of miR-200a mimic and inhibitor for control. We found that the AKT phosphorylation level elevation in response to insulin was not that obvious compared with that in insulin-resistant cells (Figure 5c). In conclusion, miR-200a mediated a substantial amelioration of insulin resistance caused by hyperinsulinemia in diabetes.

miR-200a inhibited Rheb expression and caused a series of change in glucose metabolism in post-DJB rats

After demonstrating that miR-200a targets Rheb *in vitro*, we examined whether miR-200a targets Rheb and inhibits Rheb expression *in vivo* and whether glucose homeostasis differs after transfection with a miR-200a inhibitor and mimic. Lentivirus encoding miR-200a inhibitor ($n=5$) or vector ($n=5$) were injected via the caudal vein 4 weeks before DJB. After lentivirus injection and DJB, hepatic miR-200a expression reduced by 90% in DJB +miR-200a inhibitor group (Figure 6a). Then we conducted OGTT and ITT, and measured insulin and GLP-1 levels. When glucose homeostasis was challenged, DJB rats injected with miR-200a inhibitor displayed an obviously higher glucose level at all time points in the OGTT result (Figure 6a). Insulin-stimulated glucose clearance test indicated that worse glucose clearance over the initial 30 min in the lentivirus-injected group compared to in the controls (Figure 6a). In post-DJB rats with miR-200a inhibition, the effect of bariatric surgery on insulin resistance was compromised. No significant alterations in plasma insulin and GLP-1 levels were observed (Figure 6a).

Rheb expression increased again in DJB rats injected with an miR-200a-inhibitor lentivirus, confirming that miR-200a targets Rheb *in vivo*. In the DJB+miR-200a inhibitor group, the Rheb/mTOR cassette was upregulated, and IRS1/2 tyrosine and AKT serine phosphorylation was reduced (Figure 6b). The serine phosphorylation of IRS2 remained unchanged. IHC staining confirmed that Rheb was obviously higher in the DJB+miR-200a inhibitor group than in the DJB+vector group (Figure 6c). PEPCK and G6Pase were significantly elevated in DJB+miR-200a inhibitor group (Figure 6g).

Also we injected lentivirus encoding miR-200a mimic ($n=5$) or vector in DM ($n=5$) rats. The miR-200a level increased to fourfolds after injection. DM rats injected of miR-200a mimic showed lower blood glucose level both in OGTT and ITT, but no difference was seen in insulin and GLP-1 level (Figure 6d). In the DM+miR-200a mimic group, the Rheb/mTOR cassette was downregulated, and IRS1/2 tyrosine and AKT serine phosphorylation was increased (Figure 6e). The serine phosphorylation of IRS2 remained unchanged. IHC staining confirmed that Rheb was obviously lower in the DM+miR-200a mimic group than in the DM+vector group (Figure 6f). PEPCK and G6Pase were significantly reduced in DM+miR-200a mimic group (Figure 6g).

Different miR-200a expression between DJB and SG

To elucidate whether miR-200a alteration is specific in DJB, we compared the miR-200a level in DJB ($n=5$) to sleeve gastrectomy ($n=5$), another prevalent type of bariatric surgery. qPCR analysis showed miR-200a expression remained unchanged between SG ($n=5$) and sham group ($n=5$), whereas miR-200a expression is higher in DJB than SG group (Figure 6h).

Rheb/mTOR/S6K signaling constitutively engages a negative feedback mechanism to regulate IRS1/2 expression in diabetes.¹⁶ Above all we showed a hypothesis graph demonstrating how miR-200a works in different states, DJB or diabetes (Figure 6i).

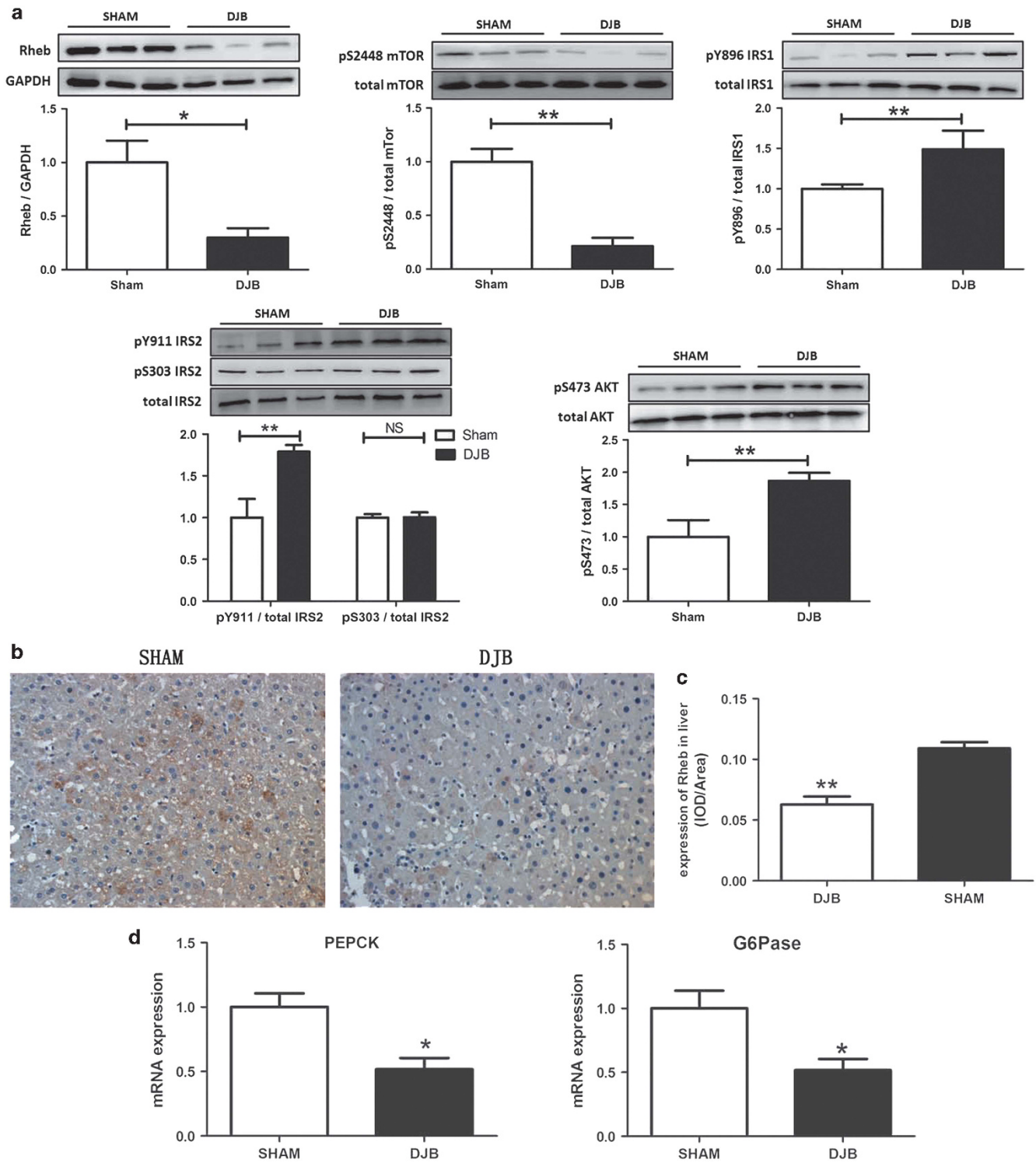


Figure 3. (a) Western blot of Rheb, mTOR, IRS1/2 and AKT expression, and their phosphorylation states in liver of DJB and sham rats at week 8 postoperatively at fed state. (b, c) IHC staining of liver showing that Rheb was clearly decreased at week 8 postoperatively. (d) mRNA expression of PEPCK and G6Pase in liver in DJB and Sham group at week 8 postoperatively at fed state, and variance between each group is similar. * $P < 0.05$, ** $P < 0.01$ according to the *t*-test.

DISCUSSION

In this study we have demonstrated a novel role for miR-200a in regulating Rheb-mediated changes in hepatic insulin resistance after DJB on diabetic rat model. We find that DJB markedly altered the expression of miR-200a, Rheb and subsequent downstream

mediators of insulin signaling. Using miR-200a mimic and inhibitor transfection, we have shown that Rheb is the target of miR-200a and significant alteration of insulin signaling can be elicited by increasing or decreasing the availability of miR-200a in insulin-resistant BRL cell line. We further verified the *in vitro* findings

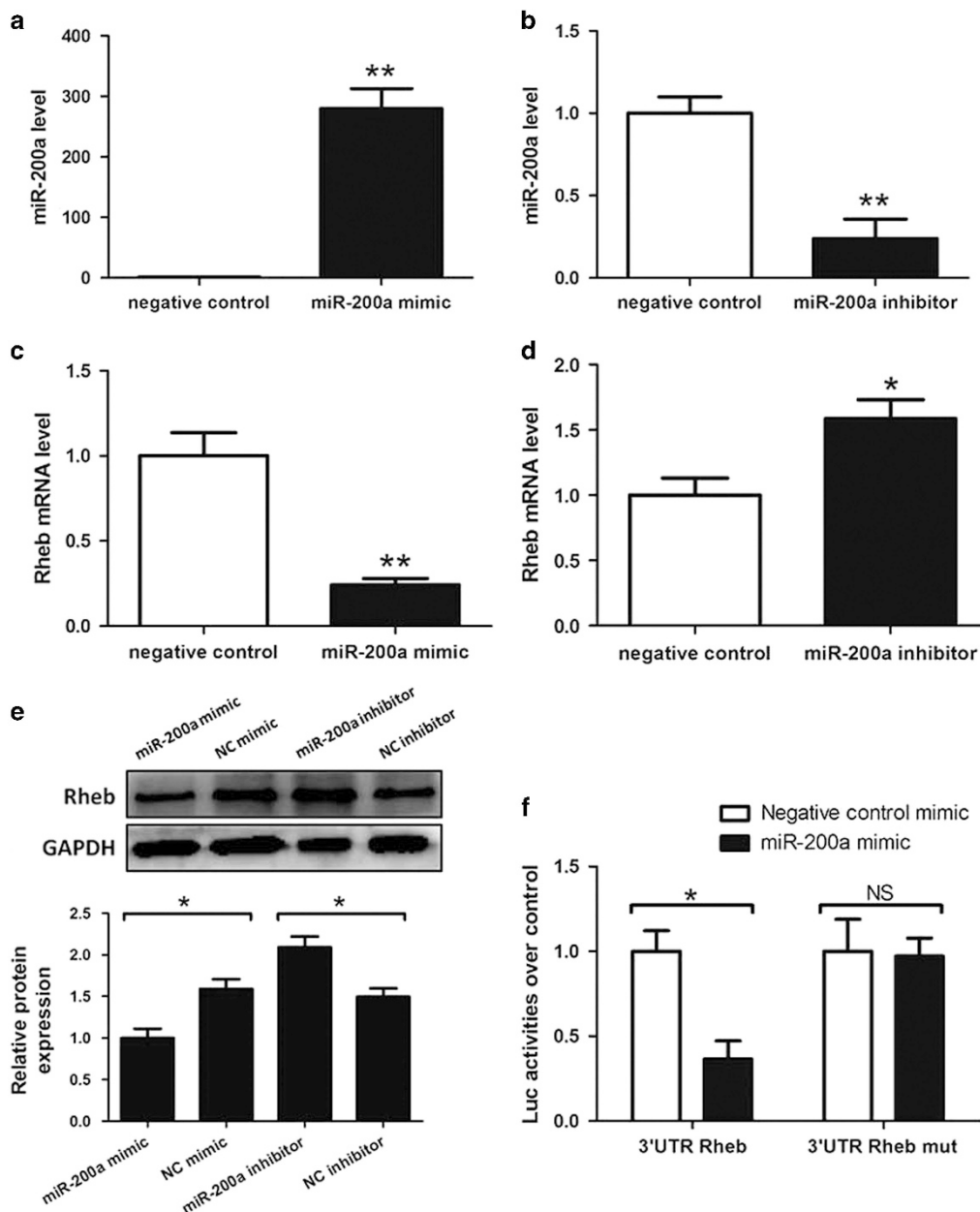


Figure 4. Rheb is a target of miR-200a. **(a, c)** Quantification of miR-200a levels. BRL cells were transfected with a negative control mimic or an miR-200a mimic for 48 h. **(b, d)** Relative quantification of Rheb mRNA levels. The data represent the mean of five independent transfections performed, \pm s.e., with $n=3$. **(e)** Analysis of Rheb protein levels. BRL cells were transfected as described above, and protein extracts were analyzed using western blot using antibodies to Rheb or to GAPDH. **(f)** The interaction between the miR-200a and 3'UTR of Rheb mRNA. NS, not significant, * $P < 0.05$, ** $P < 0.01$, and variance between each group is similar.

in vivo, by injecting lentivirus encoding miR-200a inhibitor and mimic via caudal vein in diabetic rat model before or after DJB. The role of miR-200a regulated, Rheb-mediated amelioration of hepatic insulin resistance after DJB in diabetic animals has not been reported earlier.

Rheb, a member of the Ras-like family of GTPases, is an essential component of the insulin/mTOR signaling pathway, that elicits several insulin actions, such as glucose utilization. Inactivation of the Rheb/mTOR/S6K pathway imposes a negative feedback program that fortifies IRS-dependent processes, such as insulin-mediated glucose transporting.³³ The down-regulation of downstream mediators of the IRS1-dependent insulin pathway is termed insulin resistance *in vivo*. Diabetes is characterized by insulin resistance, which represents

hyperinsulinemia and a low sensitivity of glucose-utilizing organs to insulin.⁸

In recent years, microRNAs have emerged as crucial regulators of a variety of important developmental, homeostatic and pathogenic pathways. Although several microRNAs have been implicated in various disease processes, only a few have been reported to be related to insulin resistance and bariatric surgery. It has been reported that many microRNAs, which could potentially function as a class of hormones,³⁴ contribute substantially to the beneficial effect of bariatric surgery. DJB-altered liver-produced miRNAs remarkably in a diabetic Wistar rat model. The first part of our study of a DJB and sham-operated animal model revealed that 12 miRNAs were highly dysregulated. Among these, four miRNAs (miR-29a,³⁵ miR-29c,³⁶ miR-200a^{37,38} and miR-194^(ref. 39)) were

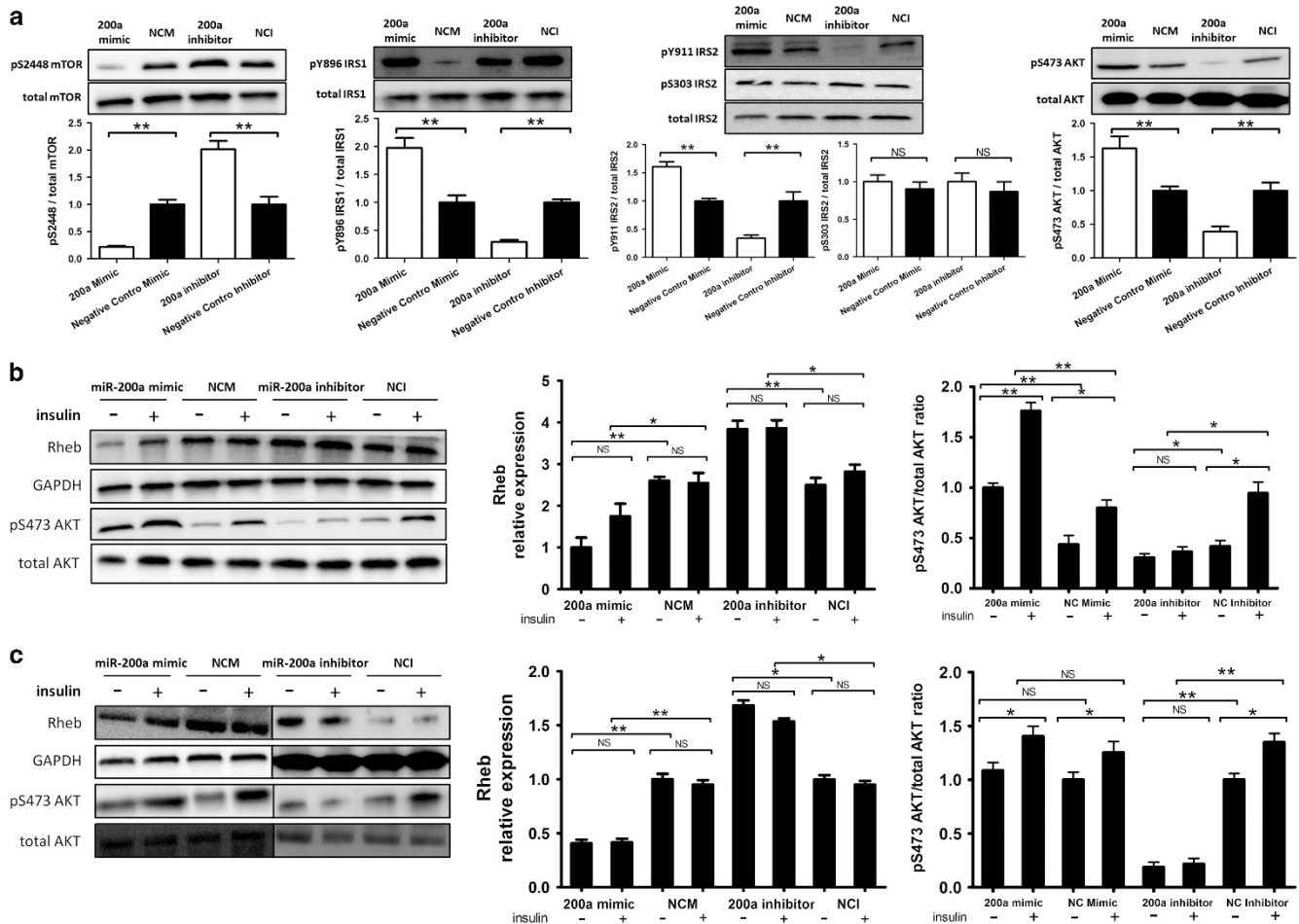


Figure 5. The effect of miR-200a on the phosphorylation level of downstream mediators in insulin-resistant BRL cell line. **(a)** Analysis and quantification of mTOR, IRS1/2 and AKT phosphorylation. **(b, c)** Analysis and quantification of Rheb and pS473-AKT-phosphorylation in response to insulin in insulin-resistant cells **(b)** or normal cells **(c)**. The data correspond to three independent experiments, each of which performed in duplicate, \pm s.e., with $n=5$. NS, not significant, $*P < 0.05$, $**P < 0.01$ and variance between each group is similar.

reported previously and our results are consistent with those findings. Five of the miRNAs (miR-27a, miR-23b, miR-365, miR-26b and miR-7i) represent miRNAs that are newly identified as relevant to diabetes.

Bariatric surgery rapidly improves glucose tolerance and reverses insulin resistance in diabetes.⁴⁰ DJB is a perfect model for studying gastric bypass due to the substantial improvement of insulin resistance in diabetic Wistar rats.⁵ As we know, high-fat diet may cause low-grade inflammation and endoplasmic reticulum stress, leading to hepatic insulin resistance.⁴¹ STZ is particularly toxic to pancreas beta cells and low dose of STZ cause relatively insufficient insulin production. Expression of miR-200a during diabetes induction shows that deduction of miR-200a is mainly due to liver inflammation and ER stress not the functional status of pancreas. Glucose metabolism is improved 4 weeks after DJB, whereas the expression of miR-200a was significantly elevated at 2 weeks after DJB which is previous to the alteration of glucose homeostasis. This suggests miR-200a initiates the amelioration of diabetes. The insulin level remains unchanged after DJB while OGTT and ITT show better results, suggesting amelioration of insulin resistance does happen. In hepatocytes, insulin signaling reportedly has an important role in glycogen synthesis because insulin suppresses the gene expression of PEPCK and G6Pase, the rate-limiting enzymes of gluconeogenesis.^{42,43} Using qPCR, we found that PEPCK and G6Pase were downregulated after DJB and

alteration of miR-200a, suggesting neoglucogenesis was suppressed. Also tyrosine phosphorylation of IRS1/2 is reported to be relevant to the insulin sensitivity while serine phosphorylation of IRS2 mediate the disruption of insulin signaling in onset of insulin resistance in hepatocytes.⁴⁴ Our data shows amelioration of insulin resistance mediated by DJB and miR-200a is dependent on tyrosine phosphorylation of IRS1/2, whereas independent of serine phosphorylation of IRS2.

We then developed *in vitro* experiments to demonstrate miR-200a regulation of Rheb in basal condition (Figure 4) and in insulin-resistant condition (Figure 5). miR-200a could elicit altered insulin signaling by targeting Rheb. Interestingly we found that miR-200a mimic could cause more obvious increase of insulin sensitivity in insulin-resistant cells than in normal cells. In normal cells the basal level of miR-200a is relatively high and the Rheb/mTOR cassette is already at turn-off status. Transfection of miR-200a will not work under this condition. However in insulin-resistant cells, Rheb/mTOR cassette is already activated, so the transfection of miR-200a mimic could inactivate the feedback Rheb/mTOR cassette by targeting Rheb.

The lentivirus transfection of miR-200a confirmed that miR-200a could influence the glucose homeostasis remarkably, but the mechanism by which DJB leads to upregulation of miR-200a remains unclear. DJB is an experimental surgical technique that excludes the duodenum and proximal jejunum from nutrient

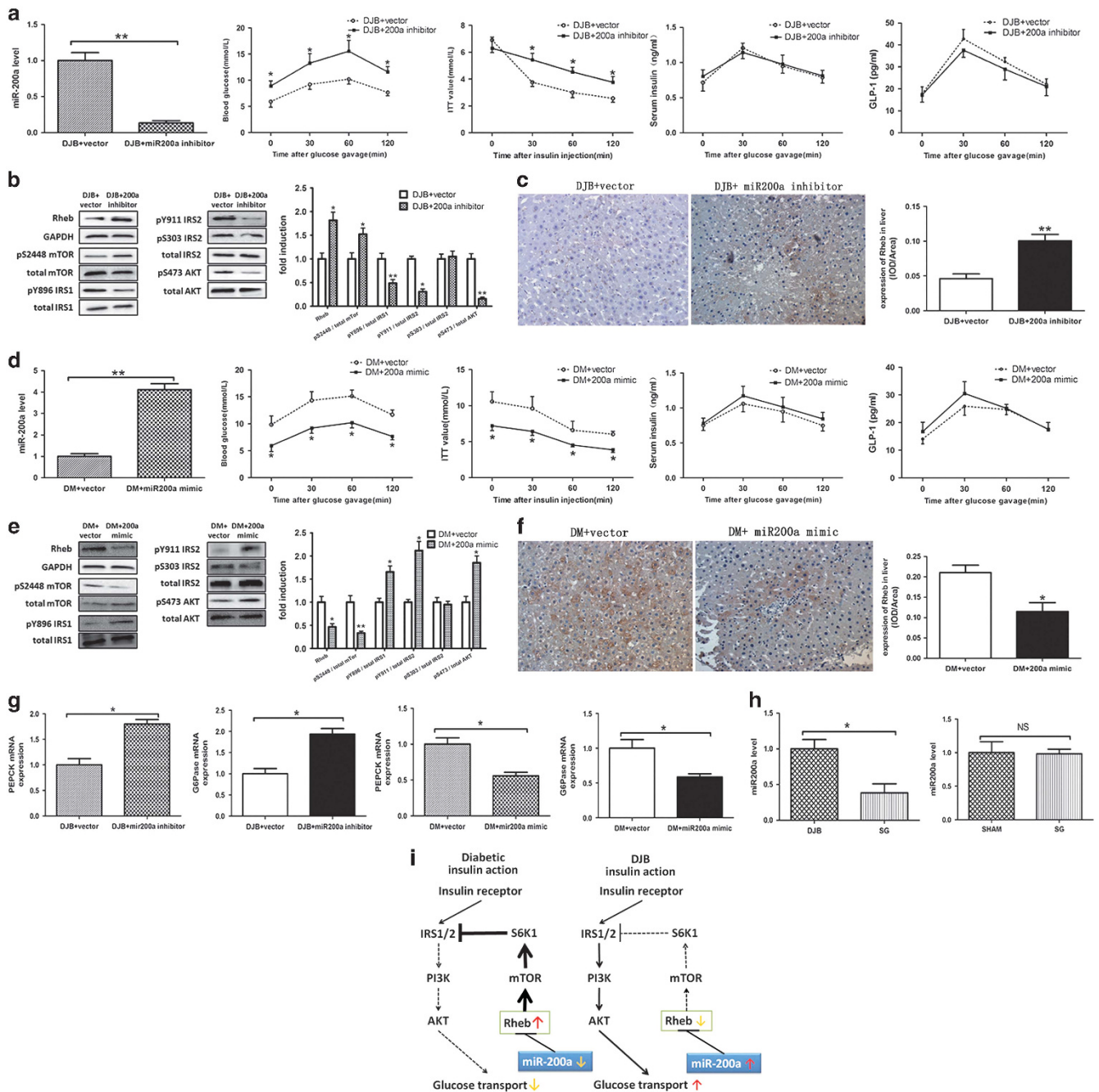


Figure 6. (a) Hepatic expression of miR-200a in DJB+miR-200a inhibitor and DJB+vector, the effect of an miR-200a inhibitor on the oral glucose tolerance test, the insulin tolerance test, serum insulin level and GLP-1 level. (b) Western blot analysis and quantification of the Rheb/mTOR cassette and the insulin pathway in liver of DJB+vector or DJB+miR-200a inhibitor. (c) Immunohistochemical analysis of Rheb in the liver of DJB+vector or DJB+miR-200a inhibitor. (d) Hepatic expression of miR-200a in DM+miR-200a mimic and DM+vector, the effect of an miR-200a mimic on the oral glucose tolerance test, the insulin tolerance test, serum insulin level and GLP-1 level. (e) Western blot analysis and quantification of the Rheb/mTOR cassette and the insulin pathway in liver of DM+miR-200a mimic and DM+vector. (f) Immunohistochemical analysis of Rheb in the liver of DM+miR-200a mimic and DM+vector. (g) mRNA expression of PEPCK and G6Pase in DJB+miR-200a inhibitor and DJB+vector. (h) Different expression of miR-200a in SG and DJB, SG and Sham. (i) Hypothesis graph. NS, not significant, * $P < 0.05$, ** $P < 0.01$ and variance between each group is similar.

transit, lowers glucose concentrations in diabetic rats. Given that DJB redirects and enhances nutrient flow into the jejunum, we need to address whether jejunal nutrient sensing is the cause that mediates miR-200a elevation. We employed another model of bariatric surgery, SG, which does not involve nutrients bypass and subsequently enhanced jejunal nutrients sensing. We found that

hepatic miR-200a level remained unchanged after SG, suggesting that enhanced nutrient flow into the jejunum is the cause of hepatic miR-200a elevation after DJB.

Metabolic disease and malignancy are thought to share common biological mechanisms.⁴⁵ Likewise, many DM-associated genes are involved in tumorigenesis.^{46,47} miR-200a is a further example of an

miRNA that regulates both metabolic disease and malignancy; miR-200a is linked to human hepatocellular carcinoma³⁷ and renal fibrogenesis in the diabetic kidney.³⁸ In our study, miR-200a was found to have a crucial role in the amelioration of insulin resistance in bariatric surgery, a finding that shows that cancer-causing miRNAs are also important in metabolic disease.

In conclusion, we demonstrated that DJB significantly modified the miRNA profiles of Wistar rats, especially the levels of miR-200a, resulting in a substantial amelioration of insulin resistance. We were able to provide, for the first time, an accurate explanation of the crosstalk between miRNAs and the insulin signaling pathway in bariatric surgery. Our study highlights the value of microRNA and opens a new direction to further understand the fundamental mechanisms associated with bariatric surgery and potential therapeutic targets for obesity and diabetes treatment.

CONFLICT OF INTEREST

The authors declare no conflict of interest.

ACKNOWLEDGEMENTS

This work was supported by the National Natural Science Foundation of China (Nos. 81270888/H0713, 81070642/H0713, 81370496/H0308 and 81300286/H0308).

AUTHOR CONTRIBUTIONS

SY Hu and W Guo were responsible for study conception and design, analyses and interpretation of the data and drafting of the manuscript. HF Han, YM Wang, X Zhang, SZ Liu and GY Zhang advised on the study concept, conducted specific analyses and critically revised the manuscript.

REFERENCES

- 1 Yach D, Stuckler D, Brownell KD. Epidemiologic and economic consequences of the global epidemics of obesity and diabetes. *Nat Med* 2006; **12**: 62–66.
- 2 Ashrafian H, Bueter M, Ahmed K, Suliman A, Bloom SR, Darzi A *et al*. Metabolic surgery: an evolution through bariatric animal models. *Obes Rev* 2010; **11**: 907–920.
- 3 Zhang H, DiBaise JK, Zuccolo A, Kudrna D, Braidotti M, Yu Y *et al*. Human gut microbiota in obesity and after gastric bypass. *Proc Natl Acad Sci USA* 2009; **106**: 2365–2370.
- 4 Li JV, Ashrafian H, Bueter M, Kinross J, Sands C, le Roux CW *et al*. Metabolic surgery profoundly influences gut microbial-host metabolic cross-talk. *Gut* 2011; **60**: 1214–1223.
- 5 Sun D, Wang K, Yan Z, Zhang G, Liu S, Liu F *et al*. Duodenal-jejunal bypass surgery upregulates the expression of the hepatic insulin signaling proteins and the key regulatory enzymes of intestinal gluconeogenesis in diabetic goto-kakizaki rats. *Obes Surg* 2013; **23**: 1734–1776.
- 6 Li M, Li H, Zhou Z, Zhou Y, Wang Y, Zhang X *et al*. Duodenal-jejunal bypass surgery ameliorates glucose homeostasis and reduces endoplasmic reticulum stress in the liver tissue in a diabetic rat model. *Obes Surg* 2013; **11**: 1734–1742.
- 7 Shah OJ, Wang Z, Hunter T. Inappropriate activation of the TSC/Rheb/mTOR/S6K cassette induces IRS1/2 depletion, insulin resistance, and cell survival deficiencies. *Curr Biol* 2004; **14**: 1650–1656.
- 8 DeFronzo RA, Simonson D, Ferrannini E. Hepatic and peripheral insulin resistance: a common feature of type 2 (non-insulin-dependent) and type 1 (insulin-dependent) diabetes mellitus. *Diabetologia* 1982; **23**: 313–319.
- 9 He L, Hannon GJ. MicroRNAs: small RNAs with a big role in gene regulation. *Nat Rev Genet* 2004; **5**: 522–531.
- 10 Ebert MS, Sharp PA. Roles for microRNAs in conferring robustness to biological processes. *Cell* 2012; **149**: 515–524.
- 11 Chuang JC, Jones PA. Epigenetics and microRNAs. *Pediatr Res* 2007; **61**: 24–29.
- 12 Bartel DP. MicroRNAs: target recognition and regulatory functions. *Cell* 2009; **136**: 215–233.
- 13 Ørom UA, Lund AH. Experimental identification of microRNA targets. *Gene* 2010; **451**: 1–5.
- 14 Villeneuve LM, Natarajan R. The role of epigenetics in the pathology of diabetic complications. *Am J Physiol Ren Physiol* 2010; **299**: 14–25.
- 15 Lorenzen J, Kumarswamy R, Dangwal S, Thum T. MicroRNAs in diabetes and diabetes-associated complications. *RNA Biol* 2012; **9**: 820–827.

- 16 Wu JH, Gao Y, Ren AJ, Zhao SH, Zhong M, Peng YJ *et al*. Altered microRNA expression profiles in retinas with diabetic retinopathy. *Ophthalmic Res* 2012; **47**: 195–201.
- 17 Kantharidis P, Wang B, Carew RM, Lan HY. Diabetes complications: the microRNA perspective. *Diabetes* 2011; **60**: 1832–1837.
- 18 Kovacs B, Lumayag S, Cowan C, Xu S. MicroRNAs in early diabetic retinopathy in streptozotocin-induced diabetic rats. *Invest Ophthalmol Vis Sci* 2011; **52**: 4402–4409.
- 19 Natarajan R, Putta S, Kato M. MicroRNAs and diabetic complications. *J Cardiovasc Transl Res* 2012; **5**: 413–422.
- 20 Yang K, Wu M, Li M, Li D, Peng A, Nie X *et al*. miR-155 suppresses bacterial clearance in *Pseudomonas aeruginosa*-induced keratitis by targeting Rheb. *J Infect Dis* 2014; **210**: 89–98.
- 21 Wang J, Yang K, Zhou L, Minhaowu Wu Y, Zhu M *et al*. MicroRNA-155 promotes autophagy to eliminate intracellular mycobacteria by targeting Rheb. *PLoS Pathog* 2013; **9**: e1003697.
- 22 He A, Zhu L, Gupta N, Chang Y, Fang F. Overexpression of micro ribonucleic acid 29, highly up-regulated in diabetic rats, leads to insulin resistance in 3T3-L1 adipocytes. *Mol Endocrinol* 2007; **21**: 2785–2879.
- 23 Xie H, Lim B, Lodish HF. MicroRNAs induced during adipogenesis that accelerate fat cell development are downregulated in obesity. *Diabetes* 2009; **58**: 1050–1057.
- 24 Ling HY, Ou HS, Feng SD, Zhang XY, Tuo QH, Chen LX *et al*. Changes in microRNA (miR) profile and effects of miR-320 in insulin-resistant 3T3-L1 adipocytes. *Clin Exp Pharmacol Physiol* 2009; **36**: 32–41.
- 25 Granjon A, Gustin MP, Rieusset J, Lefai E, Meugnier E, Güller I *et al*. The microRNA signature in response to insulin reveals its implication in the transcriptional action of insulin in human skeletal muscle and the role of a sterol regulatory element-binding protein-1c/myocyte enhancer factor 2C pathway. *Diabetes* 2009; **58**: 2555–2619.
- 26 Zhao E, Keller MP, Rabaglia ME, Oler AT, Stapleton DS, Schueler KL *et al*. Obesity and genetics regulate microRNAs in islets, liver, and adipose of diabetic mice. *Mamm Genome* 2009; **20**: 476–561.
- 27 Li ZY, Na HM, Peng G, Pu J, Liu P. Alteration of microRNA expression correlates to fatty acid-mediated insulin resistance in mouse myoblasts. *Mol Biosyst* 2011; **7**: 871–878.
- 28 Guay C, Roggli E, Nesca V, Jacovetti C, Regazzi R. Diabetes mellitus, a microRNA-related disease? *Transl Res* 2011; **157**: 253–317.
- 29 Fernandez-Valverde SL, Taft RJ, Mattick JS. MicroRNAs in beta-cell biology, insulin resistance, diabetes and its complications. *Diabetes* 2011; **60**: 1825–1856.
- 30 Kantharidis P, Wang B, Carew RM, Lan HY. Diabetes complications: the microRNA perspective. *Diabetes* 2011; **60**: 1832–1839.
- 31 Parts L, Hedman ÅK, Keildson S, Knights AJ, Abreu-Goodger C, van de Bunt M *et al*. Extent, causes, and consequences of small RNA expression variation in human adipose tissue. *PLoS Genet* 2012; **8**: e1002704.
- 32 Williams MD, Mitchell GM. MicroRNAs in insulin resistance and obesity. *Exp Diabetes Res* 2012; **2012**: 484696.
- 33 Bose SK, Shrivastava S, Meyer K, Ray RB, Ray R. Hepatitis C virus activates the mTOR/S6K1 signaling pathway in inhibiting IRS-1 function for insulin resistance. *J Virol* 2012; **86**: 6315–7337.
- 34 Cortez MA, Bueso-Ramos C, Ferdin J, Lopez-Berestein G, Sood AK, Calin GA. MicroRNAs in body fluids—the mix of hormones and biomarkers. *Nat Rev Clin Oncol* 2011; **8**: 467–544.
- 35 Zhu H, Leung SW. Identification of microRNA biomarkers in type 2 diabetes: a meta-analysis of controlled profiling studies. *Diabetologia* 2015; **58**: 900–911.
- 36 Long J, Wang Y, Wang W, Chang BH, Danesh FR. MicroRNA-29c is a signature microRNA under high glucose conditions that targets Sprouty homolog 1, and its in vivo knockdown prevents progression of diabetic nephropathy. *J Biol Chem* 2011; **286**: 11837–11885.
- 37 Petrelli A, Perra A, Cora D, Giordano S, Columbano A *et al*. MicroRNA/gene profiling unveils early molecular changes and nuclear factor erythroid related factor 2 (NRF2) activation in a rat model recapitulating human hepatocellular carcinoma (HCC). *Hepatology* 2014; **59**: 228–241.
- 38 Wang B, Koh P, Winbanks C, Coughlan MT, McClelland A, Watson A *et al*. miR-200a prevents renal fibrogenesis through repression of TGF-2 expression. *Diabetes* 2011; **60**: 280–287.
- 39 Yu Y, Chai J, Zhang H, Chu W, Liu L, Ma L *et al*. miR-194 Promotes burn-induced hyperglycemia via attenuating IGF-1R expression. *Shock* 2014; **42**: 578–656.
- 40 Rubino F, Marescaux J. Effect of duodenal-jejunal exclusion in a non-obese animal model of type 2 diabetes: a new perspective for an old disease. *Ann Surg* 2004; **239**: 1–11.
- 41 Coppari R, Bjørbaek C. Leptin revisited: its mechanism of action and potential for treating diabetes. *Nat Rev Drug Discov* 2012; **11**: 692–708.

- 42 Sakaue H, Hara K, Noguchi T, Matozaki T, Kotani K, Ogawa W *et al*. Ras-independent and wortmannin-sensitive activation of glycogen synthase by insulin in Chinese hamster ovary cells. *J Biol Chem* 1995; **270**: 11304–11309.
- 43 Shepherd PR, Nave BT, Siddle K. Insulin stimulation of glycogen synthesis and glycogen synthase activity is blocked by wortmannin and rapamycin in 3T3-L1 adipocytes: evidence for the involvement of phosphoinositide 3-kinase and p70 ribosomal protein-S6 kinase. *Biochem J* 1995; **305**: 25–28.
- 44 Valverde AM, González-Rodríguez A. Valverde and Águeda. IRS2 and PTP1B: Two opposite modulators of hepatic insulin signaling. *Arch Physiol Biochem* 2011; **117**: 105–115.
- 45 Ward PS, Thompson CB. Metabolic reprogramming: a cancer hallmark even warburg did not anticipate. *Cancer Cell* 2012; **21**: 297–308.
- 46 Doria A, Patti ME, Kahn CR. The emerging genetic architecture of type 2 diabetes. *Cell Metab* 2008; **8**: 186–200.
- 47 Voight BF, Scott LJ, Steinthorsdottir V, Morris AP, Dina C, Welch RP *et al*. Twelve type 2 diabetes susceptibility loci identified through large-scale association analysis. *Nat Genet* 2010; **42**: 579–589.



This work is licensed under a Creative Commons Attribution-NonCommercial-NoDerivs 4.0 International License. The images or other third party material in this article are included in the article's Creative Commons license, unless indicated otherwise in the credit line; if the material is not included under the Creative Commons license, users will need to obtain permission from the license holder to reproduce the material. To view a copy of this license, visit <http://creativecommons.org/licenses/by-nc-nd/4.0/>